

Communication

Allosteric Inhibitors, Crystallography and Comparative Analysis Reveal Network of Coordinated Movement Across Human Herpesvirus Proteases

Timothy M Acker, Jonathan E. Gable, Markus-Frederik Bohn, Priyadarshini Jaishankar, Michael C. Thompson, James S. Fraser, Adam R. Renslo, and Charles S. Craik

J. Am. Chem. Soc., **Just Accepted Manuscript** • DOI: 10.1021/jacs.7b04030 • Publication Date (Web): 31 Jul 2017

Downloaded from <http://pubs.acs.org> on August 7, 2017

Just Accepted

“Just Accepted” manuscripts have been peer-reviewed and accepted for publication. They are posted online prior to technical editing, formatting for publication and author proofing. The American Chemical Society provides “Just Accepted” as a free service to the research community to expedite the dissemination of scientific material as soon as possible after acceptance. “Just Accepted” manuscripts appear in full in PDF format accompanied by an HTML abstract. “Just Accepted” manuscripts have been fully peer reviewed, but should not be considered the official version of record. They are accessible to all readers and citable by the Digital Object Identifier (DOI®). “Just Accepted” is an optional service offered to authors. Therefore, the “Just Accepted” Web site may not include all articles that will be published in the journal. After a manuscript is technically edited and formatted, it will be removed from the “Just Accepted” Web site and published as an ASAP article. Note that technical editing may introduce minor changes to the manuscript text and/or graphics which could affect content, and all legal disclaimers and ethical guidelines that apply to the journal pertain. ACS cannot be held responsible for errors or consequences arising from the use of information contained in these “Just Accepted” manuscripts.

1

Allosteric Inhibitors, Crystallography and Comparative Analysis Reveal Network of Coordinated Movement Across Human Herpesvirus Proteases

Timothy M. Acker¹, Jonathan E. Gable¹, Markus-Frederik Bohn¹, Priyadarshini Jaishankar¹, Michael C. Thompson², James S. Fraser², Adam R. Renslo¹, Charles S. Craik¹

¹Department of Pharmaceutical Chemistry, University of California, San Francisco, California 94158, United States
University of California San Francisco

²Department of Bioengineering and Therapeutic Sciences, University of California, San Francisco, California 94158, United States

Supporting Information Placeholder

ABSTRACT: Targeting of cryptic binding sites represents an attractive but underexplored approach to modulating protein function with small molecules. Using the dimeric protease (Pr) from Kaposi's sarcoma-associated herpesvirus (KSHV) as a model system, we sought to dissect a putative allosteric network linking a cryptic site at the dimerization interface to enzyme function. Five cryogenic x-ray structures were solved of the monomeric protease with allosteric inhibitors bound to the dimer interface site. Distinct coordinated movements captured by the allosteric inhibitors were also revealed as alternative states in room temperature X-ray data and comparative analyses of other dimeric herpesvirus proteases. A two-step mechanism was elucidated through detailed kinetic analyses and suggests an enzyme isomerization model of inhibition. Finally, a representative allosteric inhibitor from this class was shown to be efficacious in a cellular model of viral infectivity. These studies reveal a coordinated dynamic network of atomic communication linking cryptic binding site occupancy and allosteric inactivation of KSHV Pr that can be exploited to target other members of this clinically relevant family of enzymes.

Infection by one or more of the nine herpesvirus family members is prevalent in the global population.¹ While severity of infection varies by herpesvirus subtype, these infections contribute significantly to morbidity and their effective treatment remains an important unmet clinical need. There are numerous programs aimed at developing therapeutics and elucidating new drug targets for Human herpesviridae (HHV).² One potential therapeutic strategy, of blocking the herpesvirus protease, has been validated through genetic knock-out and knock-down.³ There have been previous efforts aimed at targeting the non-canonical His-His-Ser catalytic triad that is conserved across the HHV proteases.²

We aimed to target a cryptic binding site that is accessed after rotameric state changes in Trp109 of KSHV protease (KSHV Pr).⁴ Targeting cryptic binding sites can be challenging, since endogenous ligands for these sites are not typically available, nor

is the functional effect of engaging such sites known *a priori*. Therefore, understanding how cryptic sites form, bind non-native small molecule ligands, and communicate with the rest of the protein is an active area of research, both computationally and experimentally.⁵ However, there are few experimentally validated systems where cryptic pockets have been exploited for drug design.

In this study, small molecules, kinetics, and cryogenic and room temperature x-ray crystallography were used to understand novel inhibitors that trap an inactive conformational state. Comparative analysis across the herpesvirus family identified an allosteric circuit linking distal loop regions, helix five, the cryptic binding site and the active site. We further describe the kinetic mechanism of inhibition by these compounds, elucidating a slow, two-step mechanism of inhibition. Finally, for the first time, we demonstrate cellular efficacy with an allosteric inhibitor, suggesting that engaging this cryptic binding site is a viable strategy for inhibiting herpesvirus infectivity.

The KSHV Pr dimer (Figure 1A) is known to form via a concentration dependent disorder to order transition of helix five and six that drive dimerization and catalytic competency. We previously described first-in-class allosteric inhibitors of KSHV that engage this dimerization interface by projecting two hydrophobic side chains from a rigid picolinamide scaffold (Figure 1A).⁴ This scaffold has been shown to exhibit mixed inhibition and similar results were obtained with compounds in this study (Supplemental Table 3).⁴ To more fully understand the nature of the transient, cryptic binding pocket engaged by this class of compounds, we varied the nature and connectivity of the hydrophobic side chains R¹ and R² that project into the cryptic binding site within KSHV Pr (Figure 1B, Supplemental Tables 1 and 2).

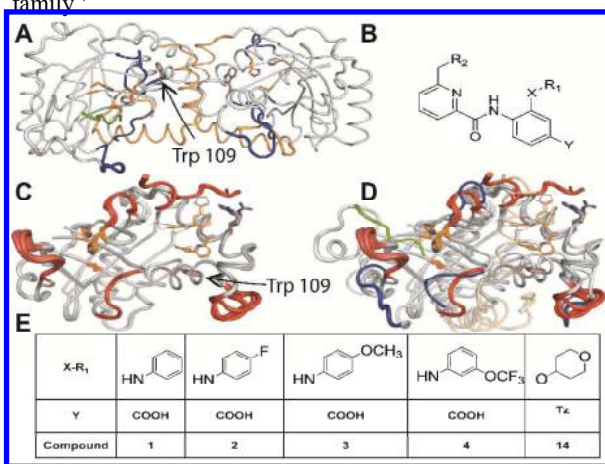
Changing the benzylic R1 side chain to aniline (X: CH₂ → NH) was well tolerated and enabled ready access to analogs with differentially substituted R1 moieties. The introduction of small substituents on the aniline ring afforded analogs with IC₅₀ values between 2.5 and 5.4 μM (Supplemental Table 1) in a biochemical

2

1 assay of KSHV Pr enzymatic activity, and were similar in potency
 2 to the original inhibitors. Somewhat improved potencies, in the
 3 sub-micromolar regime, were achieved by replacing the aniline
 4 side chain with ether or thio-ether linked aliphatic or
 5 heteroaliphatic rings at R1.

6 We next explored modification of the R2 side chain in the
 7 background of preferred alicyclic R1 groups like cyclohexyl,
 8 pyran, and thiopyran, and with further replacement of the
 9 carboxylate by the common acid bioisostere tetrazole. At R2 we
 10 prepared analogs with the original cyclohexylmethyl side chain,
 11 as well as several analogs with mono- or di-substituted benzylic
 12 side chains (Supplemental Table 2). These analogs exhibited a
 13 broader range of IC₅₀ values ranging from 0.7–13.1 μM. We
 14 found that increasing hydrophobicity of the R1 side chain
 15 improved potencies in the order pyran < thiopyran < cyclohexyl
 16 (most potent, Figure S1). By contrast, changes made to the R2
 17 side chain did not impact potency significantly (Supplemental
 18 Table 2).

19 We successfully co-crystallized five new compounds (Figure 1B,
 20 C and D) in complex with a C-terminal Δ196 construct of the
 21 protease.^{4b, 6} These X-ray crystal structures have resolution
 22 ranging between 1.8 and 2.1 Å (See Supplemental). Importantly,
 23 these structures revealed conformations of the C-terminal region
 24 and two distal loop regions, that are distinct as compared to the
 25 previously reported dimeric structure 2PBK (Figure 1B). The
 26 conformation of the oxyanion hole is rendered the active site
 27 incompetent for catalysis (Figure 1C).^{4b} It is notable that the
 28 conformation of the oxyanion hole in these experiments differs
 29 from that of an apo-monomeric protease from the alpha-
 30 herpesvirus family.⁷



31 **Figure 1.** Binding of small molecules to the cryptic binding
 32 pocket leads to coordinated rearrangements of distal sites at
 33 the protein. A. The KSHV protease dimer (PDB: 2PBK) is shown
 34 with the dimer interface helices in orange. Trp109 is shown
 35 in brown and blue and is located behind helix 5. The active site
 36 residues are shown in orange and the loop regions that adopt
 37 distinct conformations in the compound bound monomers are
 38 shown in blue. B. The small-molecule scaffold with variable R-
 39 group regions is shown, where Y is either COOH or a tetrazole
 40 (Tz). C. The cryogenic co-crystal structures solved (PDB codes:
 41 SUR3, 5UVP, 5UV3, 5UTE, 5UTN) in this study are overlaid.
 42 The dynamic loop regions are shown in red, scaled to their B-
 43 factors and the compounds are shown in orange. D. One monomer
 44 from the dimer structure (2PBK) is overlaid with a monomer
 45 from this study. Several loops from the monomeric structures, shown
 46 in red, are in distinct conformations from those of the dimeric
 47 structure shown in blue. E. The R1 groups from compounds that

are co-crystallized in this study are shown (benzyl (1), 4-F-Benzyl
 (2), 4-OCH₃-Benzyl (3), 3-OCF₃-Benzyl (4), tetrahydropyran
 (14), **Note:** R2 is cyclohexyl for each of the co-crystallized
 compounds. (This figure is enlarged in the Supplemental
 Material)

Across all molecules, the C-terminus adopts one of two
 conformations, both of which make critical but distinct H-bonds
 with the ligand. The co-crystal structure of **1** is representative of
 the first conformation (Figure S2A), which has two hydrogen
 bonding networks, one between the backbone residues (193 thru
 195) and the carboxylic acid of the molecules, and one through
 the carboxylic acid of the small molecules and the side chain
 residues of T195 and R82 (Figure S2). This conformation
 represents a significant rearrangement of the residues as compared
 to the orientation in previously reported structures. In contrast, **14**
 adopts a distinct pattern where the C-terminal residues are
 directed away from the small molecule, in a similar trajectory to
 that of the dimeric structures (Figure S2B). These two
 conformations change the overall shape of the cryptic allosteric
 pocket and the solvent accessible surface area is decreased in the
 extended conformation exemplified by **1** (Figure 2A, B).

To test the idea that these two conformations of the C-terminus
 were nearly iso-energetic, we used room temperature data

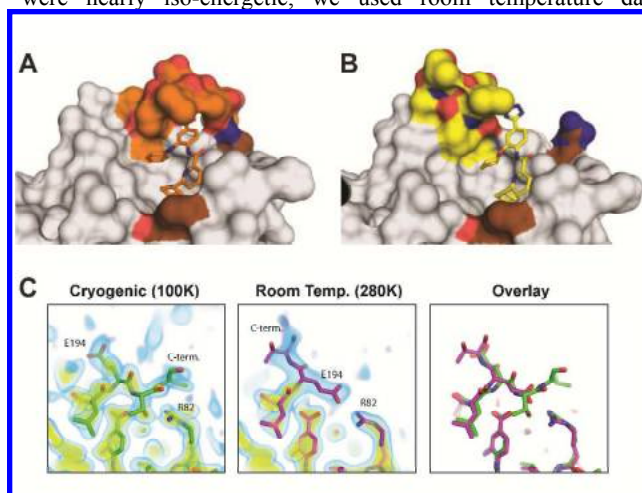


Figure 2. Distinct C-terminal conformations are identified in this
 study. A. Compound **1** cryogenic co-crystal structure with the
 surface representation shown. The orientation of the C-terminal
 residues forms a well-defined pocket that encapsulates the
 compound. B. Compound **14** cryogenic co-crystal structure with
 the surface representation shown. The orientation of the C-
 terminal residues leaves the anion exposed to solvent and is in a
 similar trajectory to that of the dimeric helices. C. Electron
 density supporting temperature-dependent conformational
 differences between structures determined at 100K and 280K
 (280K PDB codes: 5V5D, 5V5E). The leftmost column of panel
 shows an electron density map and model derived from cryogenic
 (100K, Compound 4) data, the middle panel shows maps and
 models derived from room temperature (280K, Compound 4)
 data, and the rightmost panel shows overlays of the 100K and
 280K models. The electron density maps are calculated using
 2Fo-Fc amplitudes with model phases and are contoured at 2.5σ
 (yellow) or 1.0σ (blue). A nearly 180° rotation of the φ-angle of
 Glu194 positions the C-terminus in opposite directions in each of
 the two structures, leading to a slightly different set of
 interactions stabilizing the cryptic binding site.

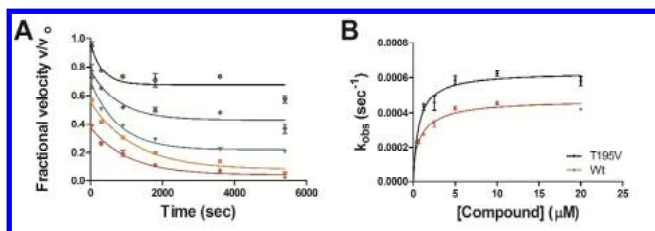
collection to avoid artifacts associated with cryo-cooling.⁸ The

3

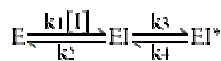
1 cryogenic and 280K structures of the protease bound to compound
 2 **4** show substantial differences where the C-terminus of the
 3 protease adopts a conformation that differs from the cryogenic
 4 structure by a 180° rotation of the ϕ -angle of Glu194 (Figure 2C).
 5 This structural rearrangement orients the C-terminus differently
 6 and alters polar interactions that form the cryptic binding site and
 7 places the carboxylate of E194 in close proximity to the
 8 guanidinium group of R82. The observation of these temperature-
 9 dependent conformational differences suggests that the protease
 10 retains considerable flexibility when bound to compound **4**. This
 11 additional conformation is similar to the conformation observed
 12 when bound to molecules such as **14**.

13 These structural observations led us to further explore the
 14 relationship between the dynamic regions within the co-crystal
 15 series developed here and across the ensemble of 24 published
 16 herpesvirus protease crystal structures. We calculated the RMSD
 17 and RMSF between the structures (Figure S3A, B). Notably, the
 18 loop regions identified above (residues 15-23, 80-100 and the
 19 oxyanion hole loop) show the largest root mean square
 20 fluctuations (RMSF) across the analysis. One way to identify
 21 whether these regions exhibiting conformational variability are
 22 coordinated is with principal component analysis (PCA) of $C\alpha$
 23 distances among these similar structures (Figure S2C). The
 24 regions showing the largest RMSF are captured by principal
 25 component one, suggesting these motions are coordinated across
 26 the structures evaluated here. The combination of allosteric acting
 27 small molecules and their co-crystal structures therefore
 28 potentially inform the identification of the link between allosteric
 29 regulation of catalysis and the overall network of atomic
 30 communication across distal regions of the protein throughout the
 31 herpesvirus family.

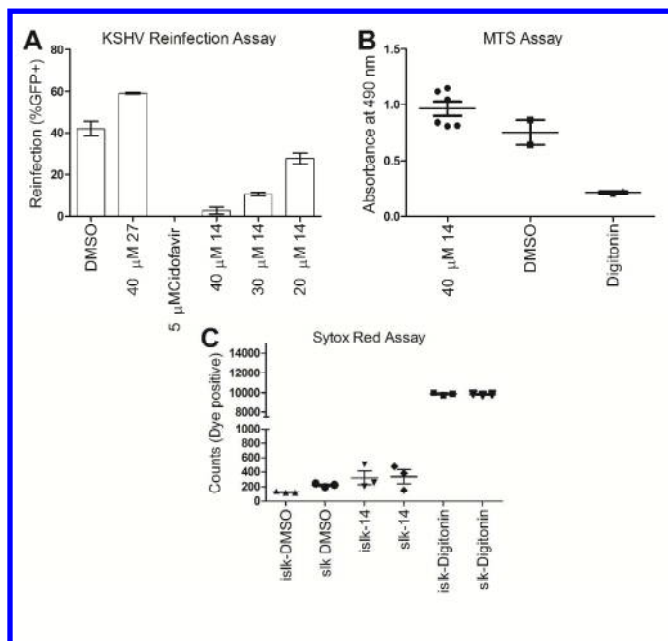
32 During our elaboration of the structure activity relationships
 33 (SAR) of compound congeners, we observed a time-dependence
 34 of inhibition with the compounds. We therefore evaluated the
 35 progress curves of the full reactions, beginning with the fractional
 36 velocity (Figure 3A). It is apparent that there is a rapid,
 37 concentration-dependent inhibition during this analysis, followed
 38 by a slow increase in inhibition over time. These observations
 39 suggest a possible two-step model of enzyme isomerization as a
 40 mechanism of inhibition. Fitting the full progress curves of the
 41 reaction for k_{obs} as a function of inhibitor concentration using the
 42 equation $[P] = v_s * t + ((v_i - v_s) / k_{obs}) (1 - \exp(-k_{obs} * t))$, where P
 43 is derived from the increase in fluorescence and t is time, reveals a
 44 hyperbolic increase in k_{obs} (Figure 4B). This observation supports



45 **Figure 3.** Compounds display slow time-dependent inhibition and
 46 two-step inhibition. **A.** The fractional velocity of the reactions
 47 shows that there is a rapid, concentration dependent inhibition
 48 followed by a slow onset to the steady-state. The curves are from
 49 a two-fold dilution scheme beginning at 25 μ M (red) and ending
 50 at 1.6 μ M (black) of compound **14**. **B.** Fitting the progress curves
 51 for k_{obs} shows a hyperbolic fit for the compounds, supporting a
 52 two-step enzyme isomerization mechanism of inhibition. The data
 53 shown are for compound **1**.



an enzyme isomerization model, e.g.
 where E is the protease monomer, EI is the initial encounter
 complex and EI^* represents an enzyme isomerization event, with
 the k_{obs} values from each concentration fitting the equation
 $k_{obs} = k_3 + ((k_4 [X]) / (K_i + [X]))$, where $[X]$ is the inhibitor
 concentration.⁹ The fitted K_i (note that K_i here is for the initial
 encounter complex) values are in good agreement with the fitted
 IC_{50} values (Compound **1**: IC_{50} 5.4 μ M, $K_i = 1.2 \pm 0.7$ μ M, $k_3 =$
 0.0003 ± 0.00008 sec^{-1} , $k_4 = 0.0001 \pm 0.00007$ sec^{-1} , Compound
14: IC_{50} 3.6 μ M, $K_i = 0.4 \pm 3$ μ M, $k_3 = 0.0003 \pm 0.001$ sec^{-1} , $k_4 =$
 0.0002 ± 0.001 sec^{-1} , Figure 5B). We note that the error associated
 with these fits is relatively large due to the very slow nature of the
 observed kinetics and the intrinsic variability in the assay system.
 We therefore chose to use pre-incubation and IC_{50} as the readout
 in our SAR campaigns, as the modest tight-binding inhibition was
 challenging to fit (See Supplemental Methods). We also verified
 the reversible nature of inhibition with rapid dilution and dialysis
 experiments (Data not shown). However, the enzyme
 isomerization model of inhibition fits with the observed structural
 rearrangements of the enzyme and the dynamic long range
 coordinated networks observed in this study. When we mutated
 T195 to V195 (Figure 3B) in order to disrupt the hydrogen
 bonding network between the side chain residue and the
 carboxylic acid of the small molecules, we observe an increase in
 the rate for k_{obs} . This observation suggests that the isomerization
 can happen faster, due to less ordering of the disordered residues,
 a phenomenon which is known to occur when shifting equilibrium
 toward the monomer.



54 **Figure 4.** Cellular evaluation of a tetrazole compound **14**. **A.**
 55 Compound **14** displays concentration dependent inhibition in
 56 re-infectivity as compared to DMSO. An inactive congener
 57 shows no inhibition of re-infectivity. Cidofavir is included as a
 58 positive control. **B.** Cell viability, as measured by MTS assay
 59 shows no significant differences between compound treated
 60 and DMSO control. Digitonin served as a positive control. **C.**
 The Sytox red assay for membrane permeability shows no
 significant differences between compound-treated and DMSO-
 treated cells for the iSLK and SLK cells.

4

Finally, the tetrazole isostere was envisioned as a candidate for cellular studies due to the distribution of the negative charge through the nitrogenous ring and a favorable cLogD (pH8.0) of 2.14. This compound was evaluated for efficacy in an established model of cellular re-infectivity using the iSLK.219 and SLK cells (Figure 4). The iSLK.219 cells are stably infected doxycycline (DOX) inducible KSHV+ cells (See Supplemental Methods). Treatment with compound **14** resulted in a dose dependent decrease in re-infectivity as measured by flow cytometry (Figure 4A, cellular EC₅₀ 23.6 μM, 95% confidence interval 22.6 to 24.6 μM). The inhibition was compound specific, with a related, biochemically inactive analog (**27**, See Supplemental) eliciting no decrease in the re-infection readout. The potential off-target cellular effects of compound **14** were evaluated using two methods. First, cell viability was assessed using a MTS assay (Figure 4B). There were no significant changes in metabolism or proliferation due to the presence of the analog as compared to the DMSO controls ($p > 0.05$, one-way ANOVA, Bonferroni post-hoc analysis). Finally, the membrane permeability of the cells was assessed using the SYTOX red assay. There was no significant increase in permeability over the DMSO controls (Figure 4C, $p > 0.05$ one-way ANOVA, Bonferroni post-hoc analysis).

Exploiting cryptic binding pockets in proteins that form protein-protein interactions presents an attractive therapeutic strategy for these challenging targets. This work advances our understanding of one such example and clearly establishes a link between cryptic pocket binding and long-range atomic communication. The opportunity to maintain the bound state via slow off rates at cryptic sites near protein interfaces otherwise requiring high surface area of binding holds the potential to allow small-molecule drug-like compounds to make further progress in modulating these challenging targets.

This study describes various cryogenic and room temperature co-crystal structures that, through comparative analysis, identify the distal regions most likely associated with the allosteric pathway of atomic communication across the herpesvirus family of proteases. Our analysis further suggests that the cryptic binding pocket shape is not rigid across the compound series assessed here, indeed temperature dependence suggests residual plasticity of distinct H-bonding patterns between the C-terminus and ligand can be further optimized to create more potent molecules. Both this plasticity and the analysis of the ensemble of all related proteases are consistent with the two-step mechanism of inhibition and induced fit type kinetics that we observe.

Finally, we establish cellular efficacy with this class of small molecules, which supports the idea that allosteric targeting of the herpesvirus proteases could be a tractable therapeutic strategy. The observed efficacy with the compounds represents a significant step forward in the pursuit of novel therapeutic strategies against human herpesviruses. We believe that the link between protein-protein interaction and the resulting allosteric networks that the herpesvirus family of proteases relies on presents an opportunity to target other viruses in a similar manner.

ASSOCIATED CONTENT

Supporting Information

The supporting information file (PDF) contains materials referenced in the above text and materials and methods for each of the experiments described above.

The Supporting Information is available free of charge on the

ACS Publications website.

AUTHOR INFORMATION

Corresponding Author

Charles S. Craik, Department of Pharmaceutical Chemistry, University of California, San Francisco, California 94158, United States University of California San Francisco. Email: Charles.Craik@ucsf.edu, Phone: 415-476-8146

Author Contributions

All authors contributed to the writing and editing of the manuscript and presentation of results.

Notes

The authors declare no competing financial interests.

ACKNOWLEDGMENT

We would like to acknowledge Christopher A. Waddling for helpful discussions, as well as Andrew Van Benschoten for assistance with room temperature data collection. We would also like to acknowledge the National Institutes of Health for funding: (R01-AI090592 to CSC, 1F32GM111012 to TMA). JEG was supported by NIH Structural Biology Training Grant GM008284 and the National Science Foundation Graduate Research Fellowship Program (1144247).

REFERENCES

1. Human Herpesviruses: Biology, Therapy, and Immunoprophylaxis. Arvin A, Gabriella, C.-F., Mocarski E, Moore, P.S., Roizman, B., Whitely, R., Yamanishi, K. editors., Ed. Cambridge University Press: Cambridge, 2007. <https://www.ncbi.nlm.nih.gov/books/NBK47376/>.
2. Gable, J. E.; Acker, T. M.; Craik, C. S. *Chem. Rev.* **2014**, 114 (22), 11382-11412.
3. Preston, V. G.; Coates, J. A. V.; Rixon, F. J. *J Virol* **1983**, 45 (3), 1056-1064.
4. (a) Shahian, T.; Lee, G. M.; Lazic, A.; Arnold, L. A.; Velusamy, P.; Roels, C. M.; Guy, R. K.; Craik, C. S. *Nat Chem. Biol.* **2009**, 5 (9), 640-646; (b) Lee, G. M.; Shahian, T.; Baharuddin, A.; Gable, J. E.; Craik, C. S. *J. Mol. Biol.* **2011**, 411 (5), 999-1016.
5. Cimermancic, P.; Weinkam, P.; Rettenmaier, T. J.; Bichmann, L.; Keedy, D. A.; Woldeyes, R. A.; Schneidman-Duhovny, D.; Demerdash, O. N.; Mitchell, J. C.; Wells, J. A.; Fraser, J. S.; Sali, A. *J. Mol. Biol.* **2016**, 428 (4), 709-719.
6. Gable, J. E.; Lee, G. M.; Jaishankar, P.; Hearn, B. R.; Waddling, C. A.; Renslo, A. R.; Craik, C. S. *Biochem* **2014**, 53 (28), 4648-4660.
7. Zuehlsdorf, M.; Werten, S.; Klupp, B.G.; Palm, G. J.; Mettenleiter, T. C.; Hinrichs, W. *PLoS Pathog.* **2015**, 11, 1-23.
8. Fraser, J. S.; van den Bedem, H.; Samelson, A. J.; Lang, P. T.; Holton, J. M.; Echols, N.; Alber, T. *Proc. Natl. Acad. Sci.* **2011**, 108 (39), 16247-16252.
9. Morrison, J. F.; Walsh, C. T. *Advances in Enzymology and Related Areas of Molecular Biology* **1988**, 61, 201-301.

5

